Journal of Molecular Liquids 264 (2018) 621–630

Contents lists available at ScienceDirect

Journal of Molecular Liquids

journal homepage: www.elsevier.com/locate/molliq

Single proton intramigration in novel 4-phenyl-3-((4-phenyl-1*H*-1,2,3-triazol-1-yl)methyl)-1*H*-1,2,4-triazole-5(4*H*)-thione: XRD-crystal interactions, physicochemical, thermal, Hirshfeld surface, DFT realization of thiol/thione tautomerism

Mohamed Reda Aouad [a], Mouslim Messali [a], Nadjet Rezki [a,b], Nabil Al-Zaqri [c], Ismail Warad [d,*]

[a] Department of Chemistry, Taibah University, 30002 Al-Madina Al-Mounawara, Saudi Arabia
[b] University of Sciences and Technology Mohamed Boudiaf, BP 1505 Oran, El M nouar, Algeria
[c] Department of Chemistry, College of Science, King Saud University, P.O. Box 2455, Riyadh 11451, Saudi Arabia
[d] Department of Chemistry, Science College, An-Najah National University, P.O. Box 7, Nablus, Palestine

ARTICLE INFO

Article history:
Received 9 April 2018
Received in revised form 12 May 2018
Accepted 19 May 2018
Available online 22 May 2018

Keywords:
XRD
DFT
Thiol⇔thione tautomerism
NMR

ABSTRACT

This study reports the synthesis of the novel crystalline 4-phenyl-3-((4-phenyl-1*H*-1,2,3-triazol-1-yl)methyl)-1*H*-1,2,4-triazole-5(4*H*)-thione compound in an excellent yield *via* multi-steps reactions. Probability of the thiol⇔thione tautomerism reaction occurrence *via* single-proton intramigration for N—H to nearby C═S was DFT-theoretically monitored. The thione tautomer isomer structure formation was supported by X-ray single crystal measurement, the lowest energy DFT-optimized structures of the molecule in gas-phase reconcile with the thionic tautomer structure solved by X-ray technique. Several physico-chemically tools like CHN-elemental analyses, FT-IR, MS, TG/DTG, XRD, UV–Vis., ^{1}H and ^{13}C NMR were served for the compound characterization. Experimental methods X-ray diffraction, NMR, UV–Vis. and FT-IR spectroscopy and their corresponding quantum-parameters were computed for their electronic and structural output. The computed Hirshfeld surface analysis (HSA) and molecular electrostatic potential (MEP) reflected the presence of several H-bonds and C—H…π (C═C) as short contacts which was detected experimentally by XRD-packing analysis.

1. Introduction

1,2,4-Triazole scaffold (belongs to an exceptionally or is typically very) stable aromatic N-heterocyclic compounds with broad applications in chemistry [1]. Triazole-based compounds exhibit fascinating biological and medicinal activities as anti-microbial, antioxidant, anti-inflammatory, analgesic, anticancer, antiviral, anticonvulsant, antitumorial and antidepressant properties [2–8]. Furthermore, 1,2,4-triazole and its derivatives can be used as ligands to coordinate several metal ions, their complexes possess rather specific magnetic-properties or peculiar molecular structures [9,10].

Intramolecular single-proton transfer process or thiol-thione tautomerization reactions have gained considerable experimental and theoretical attention due to their essential role in biological and chemical processes and its importance in understanding their mechanisms [11–13]. Several theoretical and experimental studies were performed to warble the information concerning H-transfer mechanism and properties relevant to such tautomeric-equilibrium processes [14–18]. The tautomeric single H-transfer in 1,2,4-triazole-3-thione parent to determine the thiol⇔thione favored structure controversy was concerned in several areas of biochemistry, pharmacy and chemistry [19,20].

In solid state, the intermolecular forces types critically stabilized tautomer over other, it is useful to judge by XRD the stable favored tautomeric structure form, then find conditions to convert tautomer to another one [21,22]. Quantum chemical approaches especially DFT-calculation is helpful to corroborate the XRD-solid state experimental result, stating has been extremely used to analyze experimental seen [12–18].

The present study deals with (i) synthesis, spectral, thermal and XRD-structure analysis of new 4-phenyl-3-((4-phenyl-1*H*-1,2,3-triazol-1-yl)methyl)-1*H*-1,2,4-triazole-5(4*H*)-thione compound, (ii) Compression of the DFT-optimized structure and spectral parameters with their corresponding experimental ones, (iii) The computed HSA and MPE were compared to the experimental short interactions collected by XRD measurement, (iv) The probability of single proton intra-migration in the thiol⇔thione tautomerism reaction has been

* Corresponding author.
E-mail address: warad@najah.edu (I. Warad).

https://doi.org/10.1016/j.molliq.2018.05.085
0167-7322/

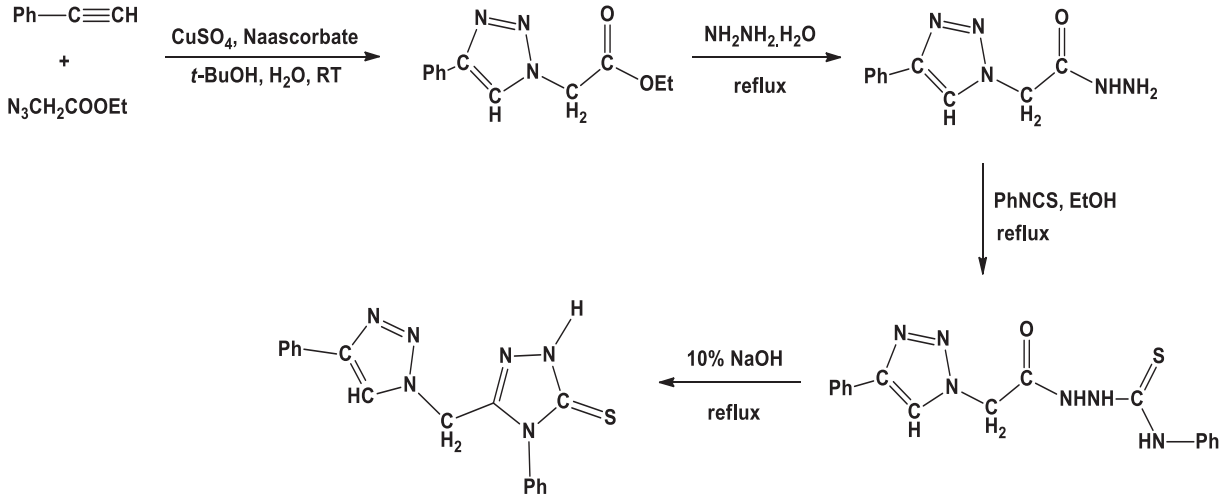

Scheme 1. Multi-step synthesis reaction to reach the desired compound.

computed and (v) the transition state structure and energy level belongs to thiol⇔thione tautomerism reaction was figured out by QST2 method of calculation.

1.1. Experimental section

1.1.1. Materials

All the chemicals were purchased from Sigma Company. The FT-IR spectrum was recorded on FTIR Affinity-1S spectrophotometer. The UV spectrum was measured with a spectrophotometer UV–visible, Finnigan 711A (8 kV) MS. TGA was conducted with a SDT-Q600, Pharmacia LKB-Biochrom 4060. ^{1}H NMR (400 MHz) and ^{13}C NMR (100 MHz) spectra was measured in DMSO at room temperature. Chemical shifts (δ) were reported in ppm, with tetramethylsilane (TMS) as an internal standard. The elemental analysis was given by using the ElementarVarrio EL analyzer.

1.1.2. Preparation of 4-phenyl-3-((4-phenyl-1H-1,2,3-triazol-1-yl) methyl)-1H-1,2,4-triazole-5(4H)-thione

A solution of *N*-phenyl-2-(2-(4-phenyl-1*H*-1,2,3-triazol-1-yl)acetyl) hydrazine-carbothioamide (10 mmol, 3.52 g) in aqueous sodium hydroxide 10% (100 mL) was refluxed for 6 h. After cooling, the reaction mixture was acidified with diluted hydrochloric acid. The precipitate formed was filtered and recrystallized from ethanol to give the desired 4-phenyl-3-((4-phenyl-1*H*-1,2,3-triazol-1-yl)methyl)-1*H*-1,2,4-triazole-5(4*H*)-thione as colorless needles in 91% yield, m.p = 269–270 °C.

IR (υ, cm^{-1}): 1265 (C═S), 1630 (C═C), 1650 (C═N), 2985 (C—H Aliph.), 3060 (C—H Ar), 3290 cm^{-1} (N—H), ^{1}H NMR (400 MHz, DMSO d_6): δ_H = 5.66 (s, 2H, CH_2), 7.32–7.76 (m, 10H, Ar—H), 8.27 (s, 1H, CH-1,2,3-triazole), 14.11 (s, 1H, N—H), ^{13}C NMR (100 MHz, DMSO d_6): δ_C = 44.3 (CH_2), 122.5 (N_2—C═C—N), 125.6, 128.3, 128.4, 129.3, 129.8, 130.1, 130.7, 133.3 (Ar—C), 146.8 (C═N), 147.4 (N_2—C═C—N), 169.1 (C═S).ESI-MS335.10 [M + 1].

1.1.3. XRD Data

A colorless needles shaped single-crystal of the compound with the dimension of 0.22 × 0.22 × 0.22 mm was selected for data collection, using Mo-K_α radiation of wavelength0.71073 Å. X-ray intensity data were collected on a Rigaku-Xta-LAB mini CCD-diffractometer with X-ray generator operating at 45 kV and 10 mA. The structure was solved by direct methods and refined by full-matrix least squares method on F^2 using *SHELXS* and *SHELXL* programs, respectively [23].

1.1.4. Computations

The DFT-calculations of the compound were carried out in the gas phase at the /B3LYP level of theory using Gaussian program [24]. HSA was performed on CRYSTAL EXPLORER 3.1 program [25].

2. Results and discussion

2.1. Synthesis

The synthesis of the targeted molecule 4-phenyl-3-((4-phenyl-1*H*-1,2,3-triazol-1-yl)methyl)-1*H*-1,2,4-triazole-5(4*H*)-thione required multi-step reactions as outlined in Scheme 1. To reach the final product in acceptable yield as thione isomer, four main steps are required; the isolated final product is soluble in ROH, DMSO and DMF.

Table 1
Crystallographic data for the compound.

Empirical formula	$C_{17}H_{14}N_6S$
Formula weight	334.4
Temperature	296(2) K
Wavelength	1.54178 Å
Reflns. for cell determination	2848
θ range for above	5.79° to 66.57°
Crystal system, Space group	Orthorhombic, P212121
Cell dimensions	a = 7.3832(3) Å, b = 14.4702(7) Å, c = 15.2806 (7) Å, α = β = γ = 90.00 (°)
Volume	1632.52(13) Å
Density, Z	1.361 Mg/m, 4
Absorption coefficient	1.849 mm
F000	696
Crystal size	0.22 × 0.22 × 0.22 mm
θ range for data collection	5.79 to 66.57 (°)
Index ranges	−8 ≤ h ≤ 8, −17 ≤ k ≤ 16, −18 ≤ l ≤ 17
Reflections collected	28,809
Independent reflections	2869 [Rint = 0.0577]
Absorption correction	Multi-scan
Refinement method	Full matrix least-squares on F 2
Data/restraints/parameters	2869/0/217
Goodness-of-fit on F 2	1.075
Final [I > 2σ(I)]	R1 = 0.0358, wR2 = 0.0944
R indices (all data)	R1 = 0.0359, wR2 = 0.0946
Largest diff. peak and hole	0.356 and −0.150 e A^{-3}

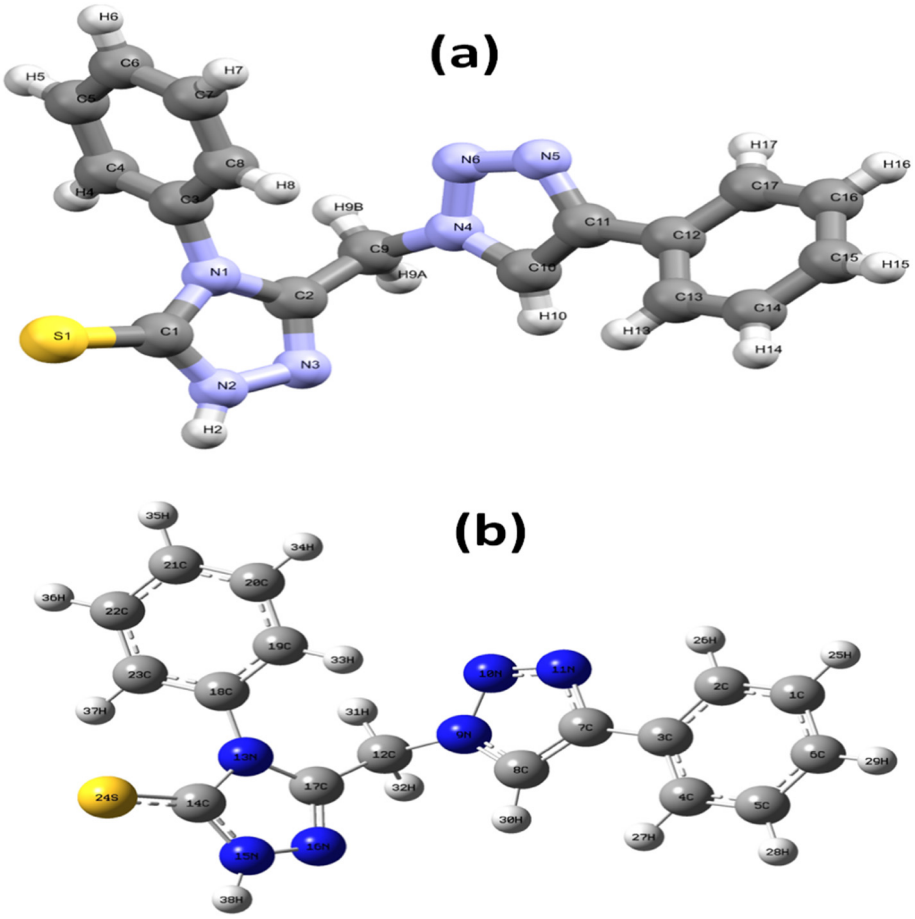

Fig. 1. (a) The XRD-POV and (b) DFT-optimized structures.

The compound was identified by CHN-analysis and several spectral like: MS, IR, UV–Vis., and ^{1}H and ^{13}C NMR. The thione-structure of the product was confirmed by X-ray single structure analysis. The thermal behavior was detected by TG/DTG. Crystal interaction was supported by HSA and MEP computed analysis (Table 1).

2.2. Crystal and DFT-optimized structure

The XRD-POV and DFT-optimized structure are illustrated in Fig. 1. Selected experimental XRD and DFT-theoretical bonds lengths and angles values are listed in Table 2. The desired compound is crystalline in the Orthorhombic space group P212121 and four molecules in the unit cell. The XRD structure confirmed the thione isomer formation, the compound is composed of 1,2,4-triazole-3-thione ring incorporating a phenyl ring on the N1 atom and a methylene group on the C2. The methylene group is also bonded to the N-4 position of the 1,2,3-triazole ring carrying a second phenyl ring on C11. The two heterocyclic rings 1,2,4-triazole-3-thione and 1,2,3-triazole rings are planar and connected together through methyl group in semi-perpendicular plane. The structure and structure parameters in this work is highly consistent with similar structure reported recently [26].

The comparison of the theoretical structural geometry with its corresponding experimental parameters determined by X-ray diffraction reflected a very high degree of harmonizes. The XRD-experimental angles and bond lengths of the compound were rewarded with DFT-theoretical ones, as seen in Fig. 2. Excellent harmony between XRD and DFT angles with $R^2 = 0.993$ graphical correlation, as plotted in Fig. 2c, the experimental and calculated angles values are very closed in their values (Fig. 2d). Very good consisting between DFT and XRD bonds lengths with $R^2 = 0.984$ graphical correlation was recorded in Fig. 2a, well XRD-DFT bonds lengths data matching was observed as in Fig. 2b.

Table 2
Selected XRD and DFT angles and bond lengths.

Bond no.	Bond type		Bond length [Å]		Angle no.	Angle type			Angle value (°)	
			XRD	DFT					XRD	DFT
1	S1	C1	1.671	1.6637	1	C1	N1	C3	124.9	125.33
2	N1	C1	1.378	1.3995	2	C1	N1	C2	107.5	107.86
3	N1	C3	1.442	1.4358	3	C3	N1	C2	127.6	126.77
4	N1	C2	1.381	1.387	4	N2	N3	C2	104.2	103.88
5	N2	N3	1.367	1.365	5	C10	N4	N6	111.3	110.82
6	N2	C1	1.336	1.3648	6	C10	N4	C9	128.4	129.17
7	N3	C2	1.302	1.3038	7	N6	N4	C9	120.3	119.97
8	N4	C10	1.345	1.3569	8	N4	C10	C11	105	104.56
9	N4	N6	1.335	1.3562	9	N4	N6	N5	106.7	107.23
10	N4	C9	1.469	1.4607	10	S1	C1	N1	128.8	130.45
11	C10	C11	1.369	1.3843	11	S1	C1	N2	127.7	127.86
12	N6	N5	1.31	1.3	12	N1	C1	N2	103.5	101.69
13	N5	C11	1.363	1.373	13	N6	N5	C11	109.6	109.87
					14	N1	C2	N3	111	111.67
					15	N4	C9	C2	111.1	112.99
					16	C10	C11	N5	107.4	107.51
					17	C10	C11	C12	130.9	130.41
					18	N5	C11	C12	121.7	122.08

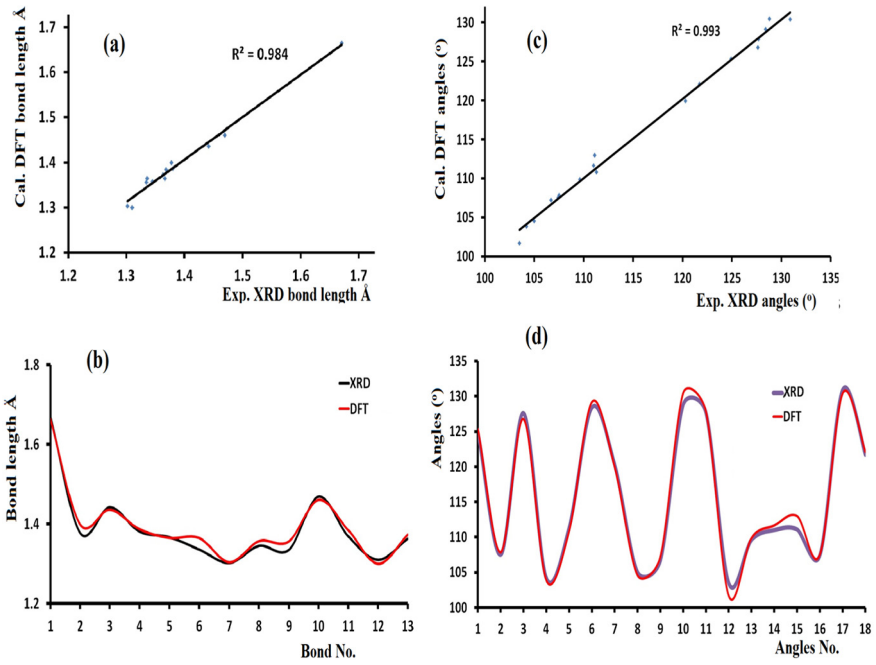

Fig. 2. (a) Graphical correlation XRD experimental bonds lengths against theoretical, (b) bond lengths *vs.* bonds No. histogram, (c) experimental angles values against theoretical graphical correlation and (d) XRD and DFT angle values *vs.* angle No. relations.

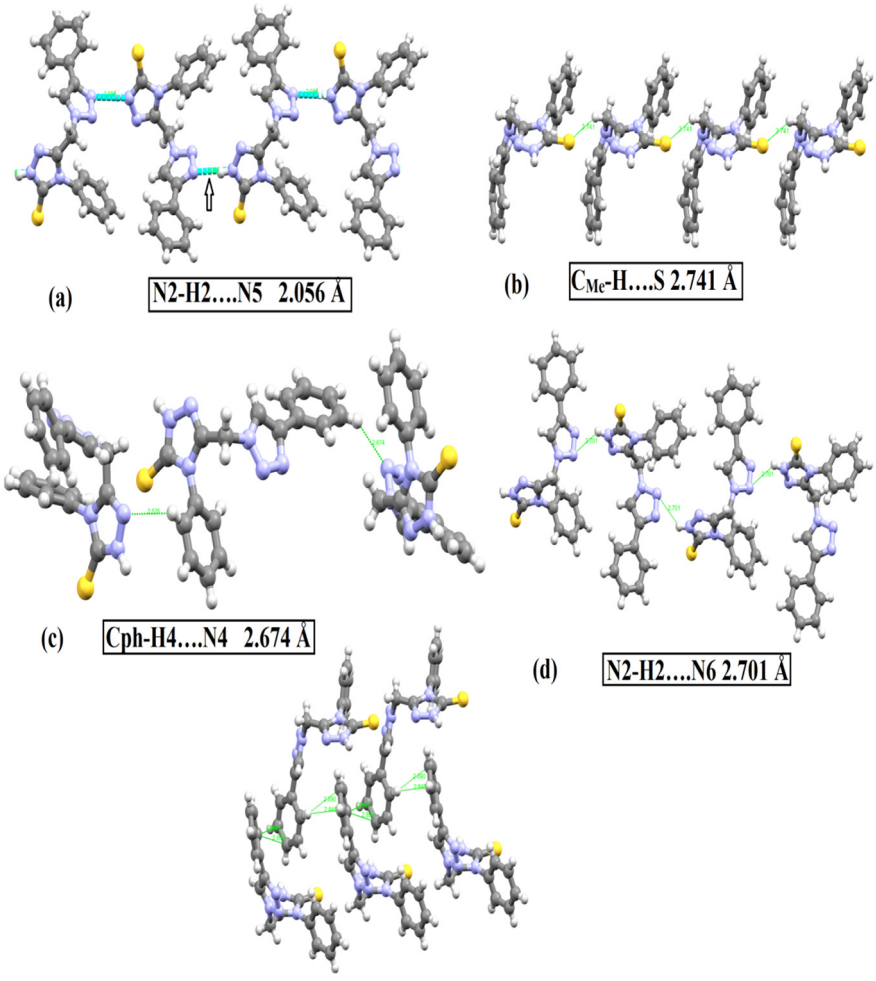

Fig. 3. View of intermolecular forces types and lengths in the crystal lattice.

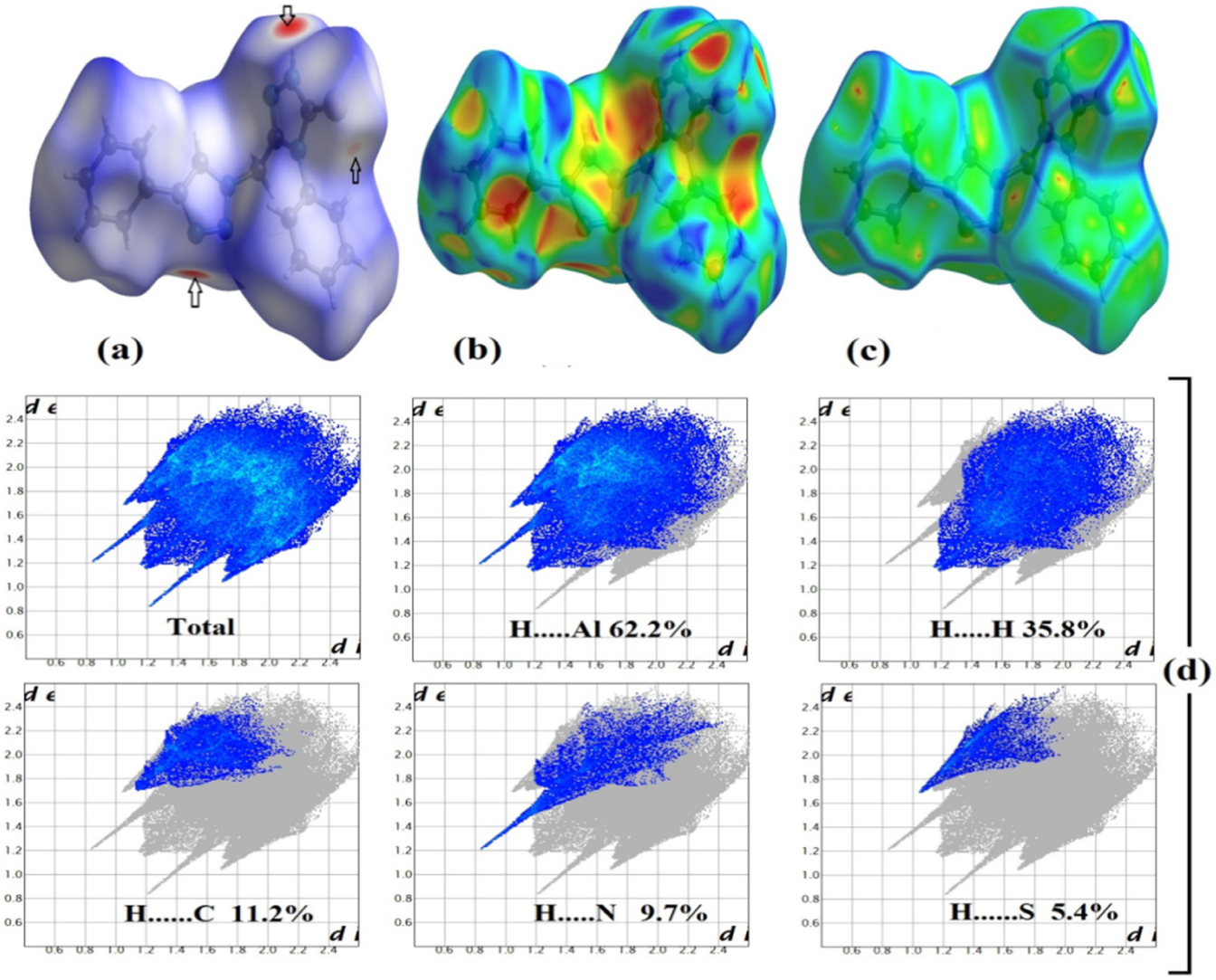

Fig. 4. (a) d_{norm} (b) shape index (c) crudeness and (d) Atom-to-atom 2D-FB plots.

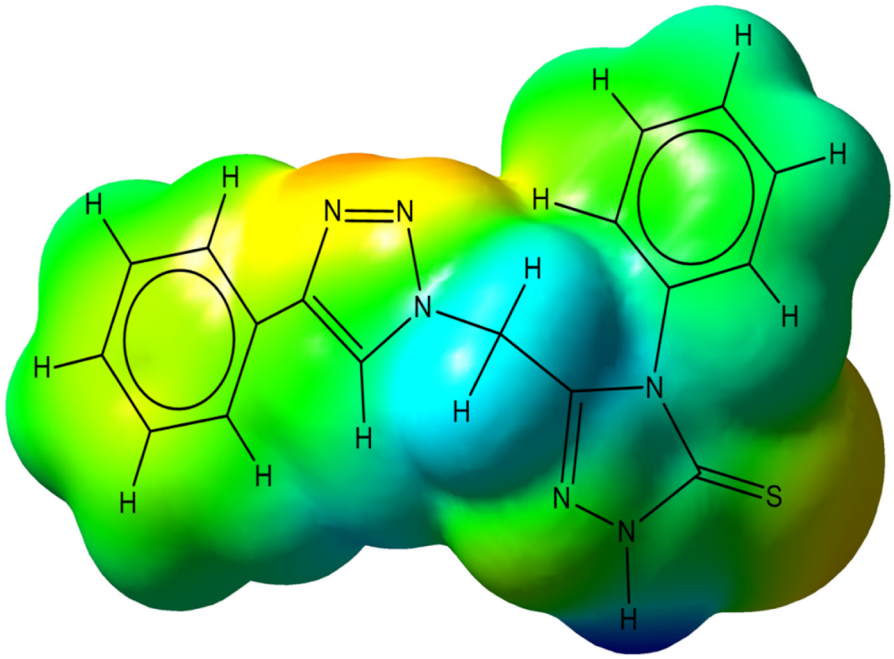

Fig. 5. (a) MEP map of the molecule.

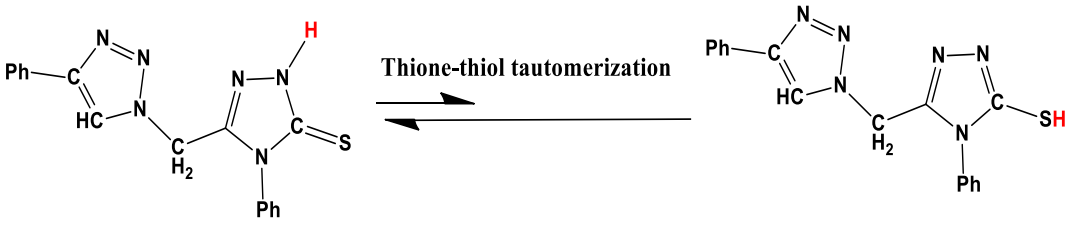

Scheme 2. Thione⇔thiol tautomerization reaction.

2.3. Crystal interactions, HSA and MEP comparison

The presence of S, N and polar H atoms (H—N) in the backbone of the compound enhanced formation of several intermolecular short contacts. Therefore, the lattice of crystalline molecule stabilized experimentally with five types of intermolecular forces, as seen Fig. 3.

Intermolecular forces were HSA computed to figure out the surface molecule red-spot positions [27–30]. Due the presence of e-rich heteroatoms like N and S together with polar H atoms three main red-spots on HAS-surface were detected (Fig. 4a–c). The biggest spot (strong contact) was detected around H—N group consisted with XRD shortest H-bond formation (N2-H2….N5 2.056 Å and N2-H2….N6 2.701 Å), another big spot reflected the formation of C_{ph}-H4….N4 with 2.674 Å H-bond. Relatively, the smallest spot was detected around the S atom supported the formation of the longer C_{Me}-H….S H-bond with 2.741 Å. 2D-Fingerprint percentage was also computed, the largest percentage contact was attributed to H….H (35.8%) and the lowest was placed to H….S (5.4%) intermolecular bonds, as in Fig. 4d.

MEP is very helpful computed technique to illustrate the charge distributions (nucleophilic and electrophilic poisons) on the functional groups as color-indicators like: blue (e-poor) < green < yellow < orange < red (e-rich). Therefore, the MEP analysis served to support the XRD and HAS interactions result. The nucleophilic positions in the molecule which indicated by red-color were placedat N═N and C═S functional groups, the deep blue (high electrophilic) was detected on proton of amine (H—N) while light blue sited to methylene protons (–CH_2–), as seen in Fig. 5. The presence of the blue (H-donor) and red colors (H-acceptor) in the desired molecule open the possibility to form different types of H-bonds, which were already observed theoretically by HAS and experimentally by XRD crystal-packing results.

2.4. Thione-thiol tautomerization

The tautomerism in organic chemistry reactions have been displayed to extended theoretical calculations using several quantum-chemical accessions [11–16]. Oxadiazole-thione heterocyclic compound live mostly in two tautomeric forms; thione and thiol tautomers. Due to the possible intra-migration of the hydrogen atom of N atom to nearby S atom, thione can be converted to thiol *vice versa* under suitable conditions [12–14], as seen in Scheme 2.

Therefore, the simultaneously tautomerization of thiol⇔thione *via* an intramolecular single proton transfer reaction has been computed in this sturdy. The thione and thiol expected structures were optimized under DFT-B3LYP/6-311G(d) level of theory. The thione isomer is computed to be the most stable form since it was confirmed by XRD.

In gas phase, the DFT-calculation consistent with the thiol⇔thione tautomerism *via* single hydrogen intra-migration reaction. The study of the reaction path for the intra-conversion between the two optimized tautomers was computed by QST2 method calculation. This method succeed in generating the structure of the transition state, where the transferred proton is in between the N and S atoms constructing pseudo four-membered heterocyclic ring with N1…H1 and S1…H1 distances 1.401 and 1.867 Å, respectively (Fig. 6(. The results indicated that the TS-structure resembles the structure of the thione tautomer rather than that of the thiol tautomer, since the transferred proton is closer to that observed for the thione than for the thiol form.

Gaseous-phase energy profiles of thiol⇔thione tautomerism through the single proton transfer process is shown in Fig. 6. The DFT-calculation reflected the thione over thiol tautomer as predominant stable isomer (zero point reference energy); the solid state XRD-solved structure is consistent with such seen. The tautomerization energy ΔE was calculated as the energy differences between the tautomers and the T.S. The $E_{T.S}$ calculated to 768.6 kJ/mol, the energy differences between the two tautomers were found to be 57.5 kJ/mol, consisted with thione tautomer as the stable isomer and thiol⇔thione possible tautomerism reaction [12–20].

2.5. CHN-elemental analyses and Mass spectroscopy

The $C_{17}H_{14}N_6S$ formula of the desired molecule was confirmed by CHN-analysis; Cald. C, 61.06; H, 4.22; N, 25.13found, C, 61.02; H, 4.18 and S, 25.07%. It also reflected MS (*m*/*z*) 335.50 $[M + 1]^+$ consisted with its theoretical molecular weight 334.60 (theoretical).

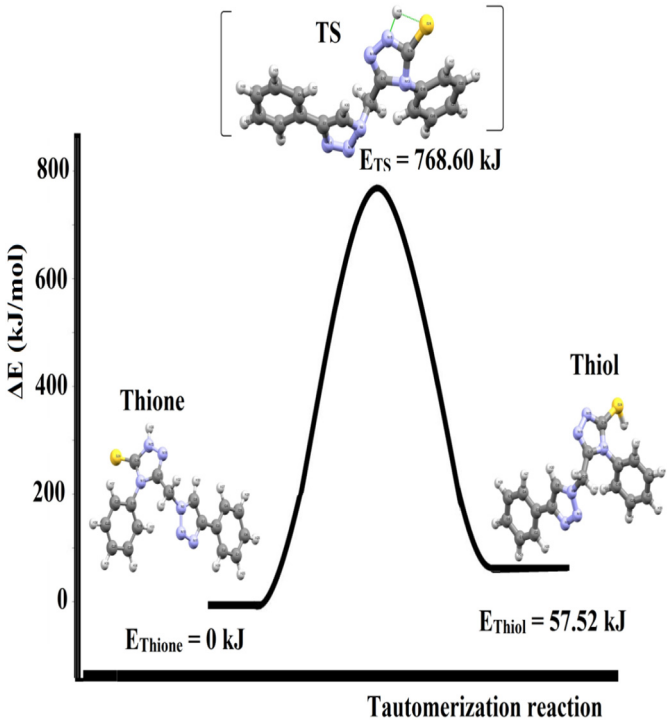

Fig. 6. Energy profiles of thiol⇔thione tautomerism.

2.6. ^{1}H NMR spectra

In addition to the X-ray crystallography, NMR result helped in the assignment of the desired structure isomer. The experimental ^{1}H NMR of the synthesized compound in DMSO *d*6 and the computed-gas phase spectra are given in Fig. 7. The ^{1}H NMR of the compound reflected the structure simplicity, the single broadpeak at 5.66 ppm is attributed to the $-CH_2-$ protons, phenyl rings protons are as expected in 7–8 ppm range, peak at 8.27 ppm is assigned to the ═CH-1,2,3-triazole proton. The diagnostic triazole-NH proton exhibited a very broad and high chemical shift signal at 14.11 ppm, thus confirming the formation of the triazole in the thione form. The broadening of the peak mainly reflected the amine proton intra-migration to the nearby sulfur atom possibility as well as its strength as acidity.

Calculated ^{1}H NMR generated by the NMR-DB [31] and ACD-LAB in gas phase were compared to experimental ^{1}H NMR as seen in Fig. 7b and c. The calculated protons chemical shifts reflected an excellent correlation with the experimental observed results. The protons chemical shifts correlation coefficients found to be 0.984 and 0.981 for NMR-DB and ACD-LAB, respectively.

2.7. The ^{13}C NMR

The presence of the triazole in the thione form was further confirmed by ^{13}C NMR analysis through the appearance of the C═S signal at δ_C 169.15 ppm. Signals at δ_C147.38 and 146.80 ppm belong to C═N and N_2—C═C—N carbons, respectively. Carbon of N_2—C═C—N resonated at δ_C 122.55 ppm, while the carbon signals characteristic of the phenyl rings are detected in122.0–134.0 ppm. The signal recorded at δ_C 44.99 ppm was assigned to the $-CH_2-$ carbon (Fig. 8).

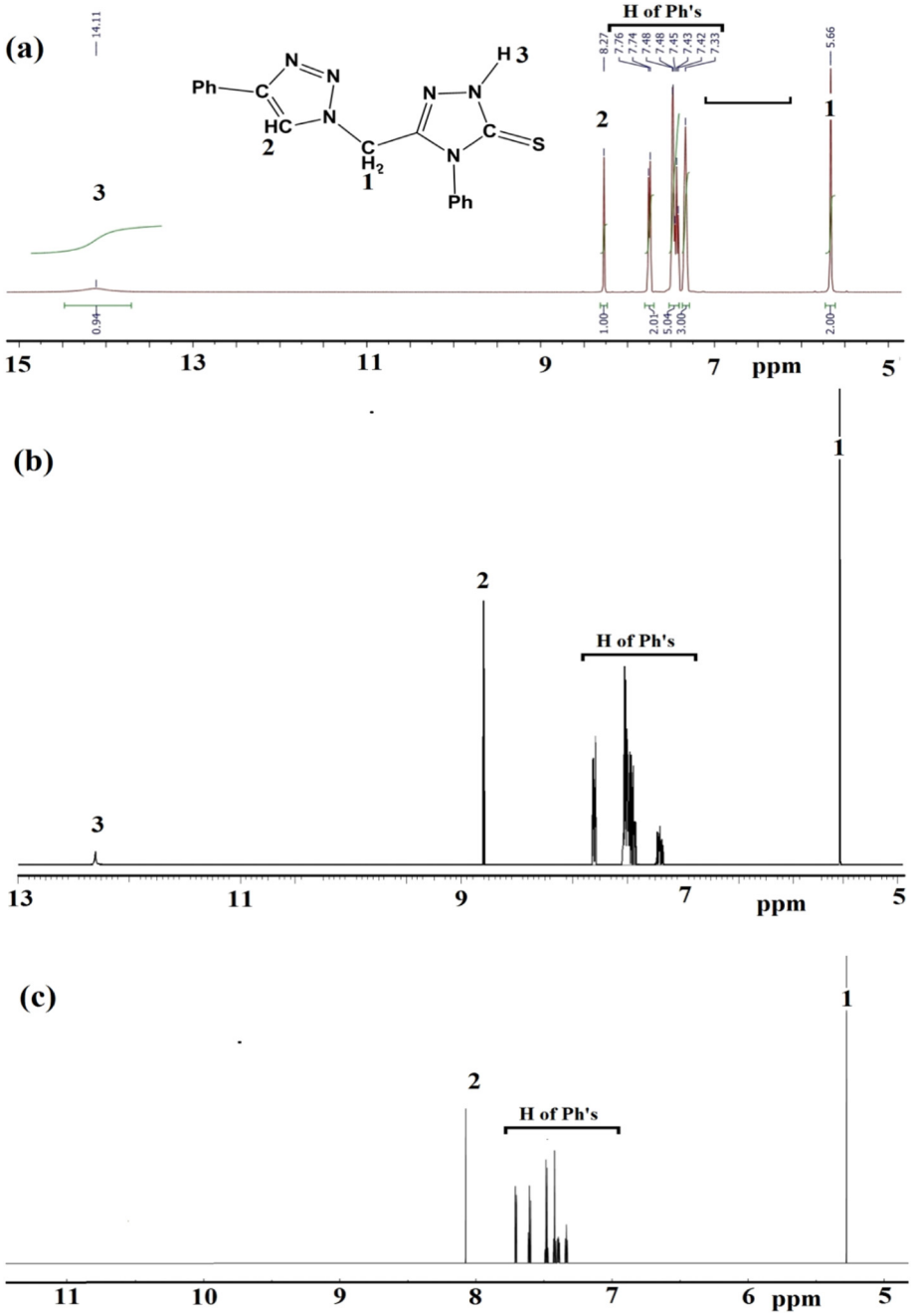

Fig. 7. ^{1}H NMR spectra, (a) experimental in DMSO *d6*, (b) calculated by ACD-LAB and (c) calculated by NMR-DB in gas phase [31].

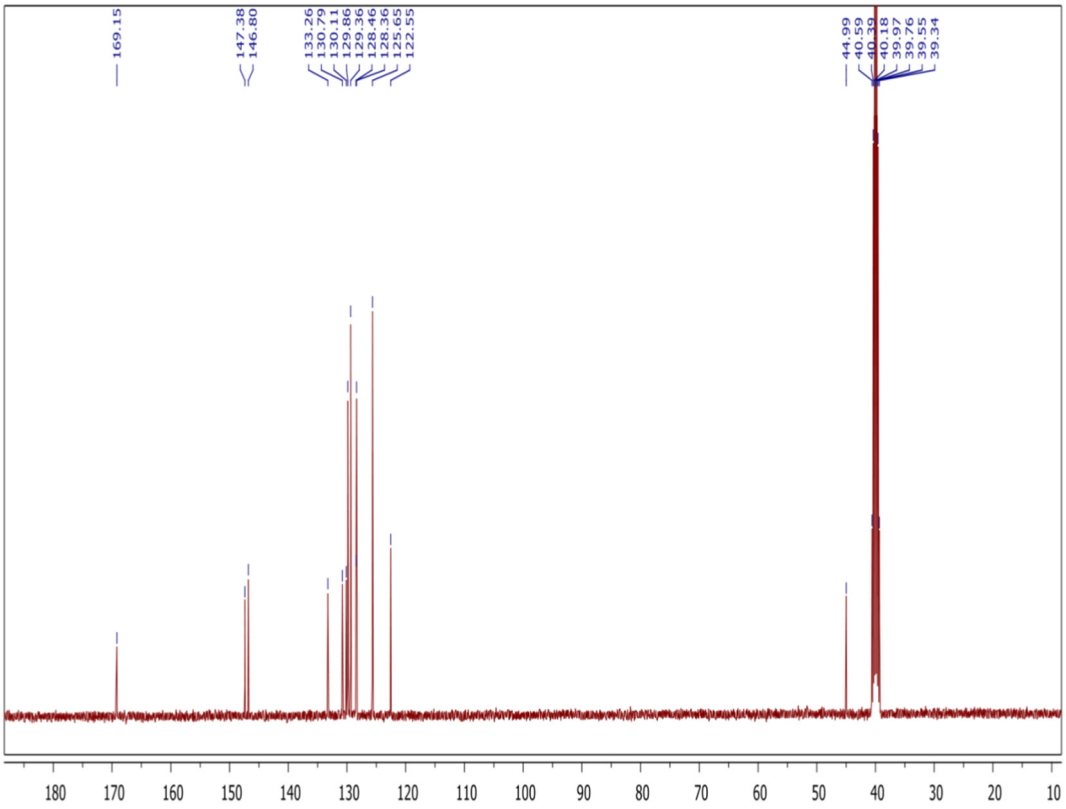

Fig. 8. ^{13}C NMR spectrum of the compound dissolved in DMSO d_6.

2.8. Exp. FT-IR and DFT-vibrational analysis

The experimental wavenumbers and DFT-theoretical vibrational spectra of the compound are shown in Fig. 9. Solid state exp. FT-IR-spectrum of the compound reflected several functional groups consistent with its molecule structure.

The main experimentally and theoretically functional groups stretching vibrations are as:

N—H: The stretching mode associated with –NH-observed exp. At 3290 cm^{-1} and DFT calculation predicted at 3650 cm^{-1}.

C_{ph}-H: Phenyl rings C—H stretching modes are generated at~3060 cm^{-1} and DFT calculation predicted at 3205 cm^{-1}.

C_{aliph}-H: Exp. methylene group ($-CH_2-$) peak observed at ~2885 cm^{-1} and DFT calculation predicted at 3105 cm^{-1}.

C═N: The exp. C═N peak observed at 1650 cm^{-1} and DFT calculation predicted at 1705 cm^{-1}.

C═C: The exp. C═C peak observed at 1630 cm^{-1} and DFT calculation predicted at 1680 cm^{-1}.

C═S: The exp. Peak observed at 1265 cm^{-1} and DFT calculation predicted at 1285 cm^{-1}.

In general, the solid state experimental FT-IR and the gas phase DFT-calculation reflected an acceptable chemical shifts correlation, as seen in Fig. 9.

2.9. UV/Vis., theoretical TD-SCF/B3LYP and HOMO, LUMO energy levels

Experimentally, the UV–visible electrons transfer of the compound dissolved in DMSO was recorded in Fig. 10a. The UV reflected broad and sharp band at $\lambda_{max} = 310$ nm, which are attributed to π-π* electron transfer. No band was recorded in the visible area,

The theoretical TD-SCF/DFT/B3LYP/6-311G(d) in DMSO reflected the compound with a sharp main-peak with $\lambda_{max} = 319$ nm (Fig. 10b), this collection is consistent with the experimental results, the small bathochromic shift ~9 nm may be due to solvent-solute interactions [21,22]. The frontier molecular orbital HOMO/LUMO was plotted as in (Fig. 10c). The E_{LUMO}, E_{HOMO} and ΔE are calculated to be −0.03563, −0.21275 and 0.17712 a.u., respectively. The highest TD-SCF/DFT theoretical λ_{max} band at 319 nm corresponded to electron transition from HOMO → LUMO and HOMO → LUMO+1 molecular orbitals.

2.10. TG-DTG

The open atmosphere TG/DTG-behavior of the compound was performed in 0 to 600 °C temperature range and under 4 °C/min. rate of heating. TG/DTG revealed the compound with high stability degree and one step thermal-decomposition mechanism (Fig. 11). The results recorded no solvent molecule detection in the solid lattice of the compound. The compound decomposed *via* abroad one step 280–380 °C range. Below 305 °C, the compound showed high degree of thermal

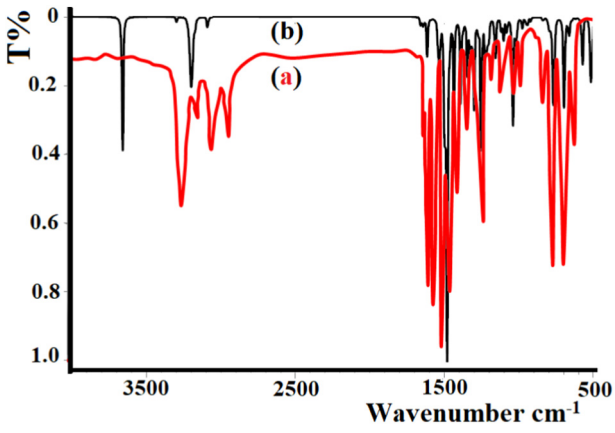

Fig. 9. (a) Exp. FT-IR and (b) DFT-vibrational spectra in the compound.

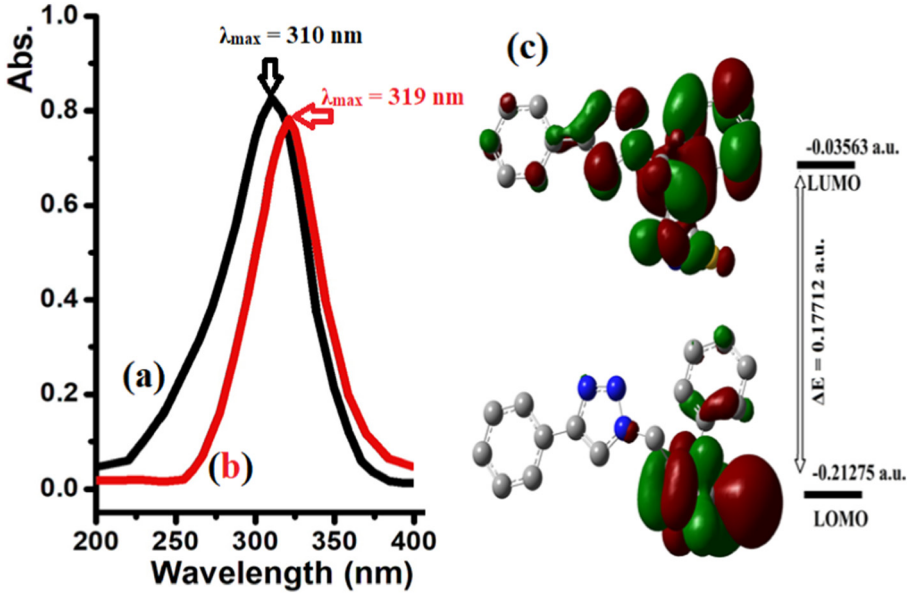

Fig. 10. (a) Exp. UV–Vis spectrum of the molecule dissolved in DMSO, (b) TD-SCF/B3LYP computed UV–visible spectrum and (c) HOMO-LUMO shapes and energy diagram in gas phase.

stability; complete decomposition was observed since no residue was collected above 380 °C.

3. Conclusions

New 1,2,3-triazole-1,2,4-triazole conjugate was synthesized and fully characterized. The compared experimental/computed analysis reflected a high degree of compatibility. TG/DTG showed a good thermal stability and the compound decomposed *via* one step thermal decomposition.

The DFT-optimized structure supported the thione tautomer as energetic favored isomer which compatible with the XRD-result. The XRD-crystal experimental packing, computed HSA and MPE agreed with N2-H2….N5, C_{Me}-H….S, C_{ph}-H4….N4, N2-H2….N6 and C_{ph}-H13. …π(C15-C16) interactions formation.

The thiol⇔thione tautomerism reaction occurrence *via* single proton intra-migration for N to the nearby S was computed, the pseudo four-membered heterocyclic ring with N1…H1….S1 transition state was detected by QST2 method of computation.

Acknowledgements

The Project was supported by the Research Centre, College of Science, King Saud University, Riyadh.

Appendix A. Supplementary material

Crystallographic data for desired compound has been deposited with the Cambridge Crystallographic Data Centre as supplementary publication number CCDC 1824847, respectively. Copies of this information may be obtained free of charge *via* www.ccdc.cam.ac.uk/conts/retrieving.html (or from the CCDC, 12 Union Road, Cambridge CB2 1EZ, UK; Fax: +44-1223-336033; e-mail: deposit@ccdc.cam.ac.uk).

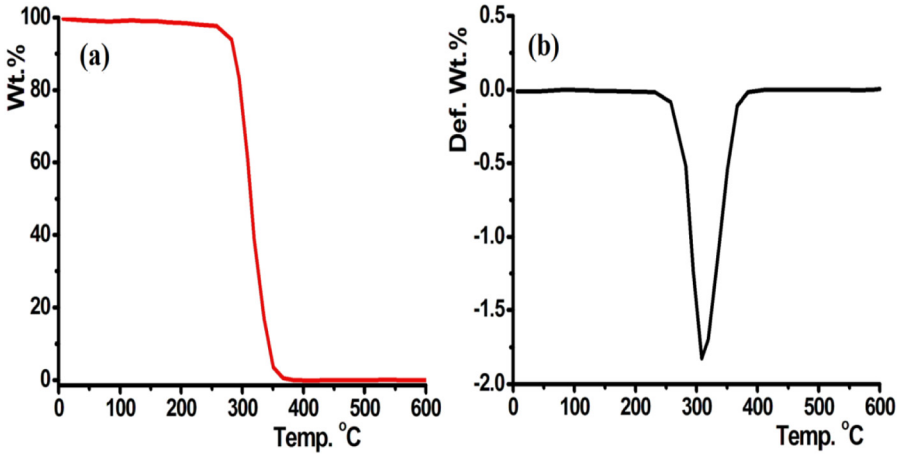

Fig. 11. (a) TG and (b) DTG curves of the compound.

References

[1] C. Temple Jr., Triazoles 1, 2, 4, in: J.A. Montgomery (Ed.), Chemistry of the Heterocyclic Compounds, 37, John Wiley & Sons, New York 1981, pp. 155–162.

[2] K. Sztanke, T. Tuzimski, J. Rzymowska, K. Pasternak, M. Kandefer-Szerszen, Synthesis, determination of the lipophilicity, anticancer and antimicrobial properties of some fused 1,2,4-triazole derivatives, Eur. J. Med. Chem. 43 (2008) 404–419.

[3] A.K. Srivastava, A. Kumar, N. Misra, P.S. Manjula, B.K. Sarojini, B. Narayana, Synthesis, spectral (FT-IR, UV-visible, NMR) features, biological activity prediction and theoretical studies of 4-Amino-3-(4- hydroxybenzyl)-1H-1,2,4-triazole-5(4H)-thione and its tautomer, J. Mol. Struct. 1107 (2016) 137–144.

[4] H. Bayrak, A. Demirbas, N. Demirbas, S.A. Karaoglu, Synthesis of some new 1,2,4-triazoles starting from isonicotinic acid hydrazide and evaluation of their antimicrobial activities, Eur. J. Med. Chem. 44 (2009) 4362–4366.

[5] Y. Ünver, K. Sancak, F. Çelik, E. Birinci, M. Küçük, S. Soylu, N.A. Burnaz, New thiophene-1,2,4-triazole-5(3)-ones: highly bioactive thiosemicarbazides, structures of Schiff bases and triazoleethiols, Eur. J. Med. Chem. 84 (2014) 639–650.

[6] S.V. Bhandari, K.G. Bothara, M.K. Raut, A.A. Patil, A.P. Sarkate, V.J. Mokale, Design, synthesis and evaluation of antiinflammatory, analgesic and ulcer- ogenicity studies of novel S-substituted phenacyl-1,3,4-oxadiazole-2-thiol and Schiff bases of diclofenac acid as nonulcerogenic derivatives, Bioorg. Med. Chem. 16 (2008) 1822–1831.

[7] M.S. Karthikeyan, Synthesis, analgesic, anti-inflammatory and antimicrobial studies of 2,4-dichloro-5-fluorophenyl containing thiazolotriazoles, Eur. J. Med. Chem. 44 (2009) 827–833.

[8] M. Koparir, C. Orek, A.E. Parlak, A. Soylemez, P. Koparir, M. Karatepe, S.D. Dastan, Synthesis and biological activities of some novel aminomethyl derivatives of 4-substituted-5-(2-thienyl)-2,4-dihydro-3H-1,2,4-triazole-3- thiones, Eur. J. Med. Chem. 63 (2013) 340–346.

[9] K. Zamani, K. Faghihi, T. Tofighi, M.R. Shariatzadeh, Synthesis and antimicrobial activity of some pyridyl and naphthyl substituted 1,2,4- triazole and 1,3,4-thiadiazole derivatives, Turk. J. Chem. 28 (2004) 95–100.

[10] W. Vreugdenhil, J.G. Haasnoot, J. Reedijk, A.L. Spek, Ferromagnetic and antiferromagnetic spin coupling in Ni4O4 cubane-type clusters with 4-amino-3,5-bis (hydroxymethyl)-1,2,4-triazole as a ligand. The X-ray structure of a new dumbbell-like double cubane cluster, Inorg. Chim. Acta 129 (1987) 205–216.

[11] N. Özdemir, D. Türkpençe, Theoretical investigation of thione-thioltautomerism, intermolecular double proton transfer reaction and hydrogen bonding interactions in 4-ethyl-5-(2-hydroxyphenyl)-2*H*-1,2,4-triazole-3(4*H*)-thione, Comput. Theor. Chem. 1025 (2013) 35–45.

[12] J.K. Lanyi, Mechanism of ion transport across membranes. Bacteriorhodopsin as a prototype for proton pumps, J. Biol. Chem. 272 (1997) 31209–31212.

[13] Y.-Q. Wang, H.-G. Wang, S.-Q. Zhang, K.-M. Pei, X. Zheng, D.L. Phillips, Resonance raman intensity analysis of the excited state proton transfer dynamics of 2-nitrophenol in the charge-transfer band absorption, J. Chem. Phys. 125 (2006) 214506–214517.

[14] H. Gökce, N. Öztürk, Ü. Ceylan, Y.B. Alpaslan, G. Alpaslan, Thiol–thione tautomeric analysis, spectroscopic (FT-IR, Laser Raman, NMR and UV–vis) properties and DFT computations of 5-(3-pyridyl)-4H-1,2,4-triazole-3-thiol molecule, Spectrochim. Acta A Mol. Biomol. Spectrosc. 163 (2016) 170–180.

[15] T.A. Mohamed, U.A. Soliman, I.A. Shaaban, W.M. Zoghaib, L.D. Wilson, Raman, infrared and NMR spectral analysis, normal coordinate analysis and theoretical calculations of 5-(methylthio)-1,3,4-thiadiazole-2(3H)- thione and its thiol tautomer, Spectrochim. Acta A Mol. Biomol. Spectrosc. 150 (2015) 339–349.

[16] S.M. Solima, M. Hagar, F. Ibid, E.H. El Ashry, Experimental and theoretical spectroscopic studies, HOMO–LUMO, NBO analyses and thione–thioltautomerism of a new hybrid of 1,3,4-oxadiazole-thione with quinazolin-4-one, Spectrochim. Acta A Mol. Biomol. Spectrosc. 145 (2015) 270–279.

[17] N. Burcu, A.N. Özdemir, O. Dayan, N. Dege, M. Koparır, P. Koparır, H. Mugelu, Direct and solvent-assisted thione–thiol tautomerism in 5-(thiophen-2-yl)-1,3,4-oxadiazole-2(3*H*)-thione: experimental and molecular modeling study, Chem. Phys. 439 (2014) 1–11.

[18] S. Pang, Y. Zhao, X. Liu, J. Xue, X. Zheng, Solvent-dependent dynamics of hydrogen bonding structure 5-(methylthio)-1, 3, 4-thiadiazole-2(3H)-thione as determined by Raman spectroscopy and theoretical calculation, Spectrochim. Acta A Mol. Biomol. Spectrosc. 171 (2017) 470–477.

[19] K.C. Hunter, L.R. Rutledge, S.D. Wetmore, The Hydrogen bonding properties of cytosine: a computational study of cytosine complexed with hydrogen fluoride, water, and ammonia, J. Phys. Chem. A 109 (2005) 9554–9562.

[20] O. Kahn, C.J. Martinez, Spin-transition polymers: from molecular materials toward memory devices, Science 279 (1998) 44–48.

[21] A. Barakat, S.M. Soliman, H.A. Ghabbour, M. Ali, A.M. Al-Majid, A. Zarrouk, I. Warad, Intermolecular interactions in crystal structure, Hirshfeld surface, characterization, DFT and thermal analysis of 5-((5-bromo-1H-indol-3-yl)methylene)-1,3-dimethylpyrimidine-2,4,6(1H,3H,5H)-trione indole, J. Mol. Struct. 1137 (2017) 354–361.

[22] A. Barakat, M. Islam, A. Al-Majid, H.A. Ghabbour, S. Atef, A. Zarrouk, I. Warad, Quantum chemical insight into the molecular structure of L-chemosensor 1,3-dimethyl-5-(thien-2-ylmethylene)-pyrimidine- 2,4,6-(1H,3H,5H)-trione: naked-eye colorimetric detection of copper(II) anions, J. Theor. Comput. Chem. 17 (2018) 1–23.

[23] G.M. Sheldrick, A short history of SHELX, Acta Cryst 64 (2008) 112–122.

[24] M.J. Frisch, G.W. Trucks, H.B. Schlegel, G.E. Scuseria, M.A. Robb, J.R. Cheeseman, J.A. Montgomery Jr., T. Vreven, K.N. Kudin, J.C. Burant, J.M. Millam, S.S. Iyengar, J. Tomasi, V. Barone, B. Mennucci, M. Cossi, G. Scalmani, N. Rega, G.A. Petersson, H. Nakatsuji, M. Hada, M. Ehara, K. Toyota, R. Fukuda, J. Hasegawa, M. Ishida, T. Nakajima, Y. Honda, O. Kitao, H. Nakai, M. Klene, X. Li, J.E. Knox, H.P. Hratchian, J.B. Cross, V. Bakken, C. Adamo, J. Jaramillo, R. Gomperts, R.E. Stratmann, O. Yazyev, A.J. Austin, R. Cammi, C. Pomelli, J.W. Ochterski, P.Y. Ayala, K. Morokuma, G.A. Voth, P. Salvador, J.J. Dannenberg, V.G. Zakrzewski, S. Dapprich, A.D. Daniels, M.C. Strain, O. Farkas, D.K. Malick, A.D. Rabuck, K. Raghavachari, J.B. Foresman, J.V. Ortiz, Q. Cui, A.G. Baboul, S. Clifford, J. Cioslowski, B.B. Stefanov, G. Liu, A. Liashenko, P. Piskorz, I. Komaromi, R.L. Martin, D.J. Fox, T. Keith, M.A. Al-Laham, C.Y. Peng, A. Nanayakkara, M. Challacombe, P.M.W. Gill, B. Johnson, W. Chen, M.W. Wong, C. Gonzalez, J.A. Pople, Gaussian 09, Gaussian Inc., Wallingford CT, 2009.

[25] S.K. Wolff, D.J. Grimwood, J.J. McKinnon, D. Jayatilaka, M.A. Spackman, Crystal Explorer 2.1, University of Western Australia, Perth, 2007.

[26] E.H. El Ashry, L.F. Awad, S.M. Soliman, M.N.A. Al-Moaty, H.A. Ghabbour, A. Barakat, Tautomerism aspect of thione-thiol combined with spectral investigation of some 4-amino-5-methyl-1,2,4-triazole-3-thione Schiff's bases, J. Mol. Struct. 1146 (2017) 432–440.

[27] I. Warad, F.F. Awwadi, M. Daqqa, A. Al Ali, T.S. Ababneh, T.M.A. AlShboul, T.M.A. Jazzazi, F. Al-Rimawie, T.B. Hadda, Y.N. Mabkhot, New isomeric Cu(NO_2-phen)$_2$Br] Br complexes: crystal structure, Hirschfeld surface, physicochemical, solvatochromism, thermal, computational and DNA-binding analysis, J. Photochem. Photobiol. B Biol. 171 (2017) 9–19.

[28] I. Warad, Y. Al-Demeri, M. Al-Nuri, S. Shahwan, M. Abdoh, S. Naveen, N.K. Lokanath, M.S. Mubarak, T.B. Hadda, Y.N. Mabkhot, Crystal structure, Hirshfeld surface, physicochemical, thermal and DFT studies of (N1E,N2E)-N1,N2-bis((5-bromothiophen-2-yl)methylene) ethane-1,2-diamine N2S2 ligand and its [CuBr(N2S2)]Br complex, J. Mol. Struct. 1142 (2017) 217–225.

[29] F. Abu Saleemh, S. Musameh, A. Sawafta, P. Brandao, C.J. Tavares, S. Ferdov, A. Barakat, A. Al Ali, M. Al-Noaimi, I. Warad, Diethylenetriamine/diamines/copper (II) complexes [Cu(dien)(NN)]Br_2: synthesis, solvatochromism, thermal, electrochemistry, single crystal, Hirshfeld surface analysis and antibacterial activity, Arab. J. Chem. 10 (2017) 845–854.

[30] I. Warad, S. Musameh, I. Badran, N.N. Nassar, P. Brandao, C.J. Tavares, A. Barakat, Synthesis, solvatochromism and crystal structure of trans-[Cu($Et_2NCH_2CH2NH_2$)$_2$.H_2O] (NO_3)$_2$ complex: experimental with DFT combination, J. Mol. Struct. 1148 (2017) 328–338.

[31] D. Banfi, L. Patiny, www.nmrdb.org: resurrecting and processing NMR spectra online, Chimia 62 (2008) 280–281.